02 May 2013, 7:00 pm - 8:30 pm

A Case History of Super-Large Scale Bridge Pile Foundation in Soft Soil

Chao Yang
Southeast University, China

Guoliang Dai
Southeast University, China

Weiming Gong
Southeast University, China

Commemorate the Legacy of Ralph B. Peck
April 29 - May 4, 2013 CHICAGO
Seventh International Conference on
Case Histories in Geotechnical Engineering
and Symposium in Honor of Clyde Baker

A CASE HISTORY OF SUPER-LARGE SCALE BRIDGE PILE FOUNDATION IN SOFT SOIL

Chao Yang
Key Laboratory for RC and PRC Structures of Education Ministry, Southeast University
Nanjing, Jiangsu-China 210096

Guoliang Dai
Key Laboratory for RC and PRC Structures of Education Ministry, Southeast University
Nanjing, Jiangsu-China 210096

Weiming Gong
Key Laboratory for RC and PRC Structures of Educati on Ministry, Southeast University
Nanjing, Jiangsu-China 210096

ABSTRACT

The Sutong Yangtze River Bridge is the longest cable-stayed bridge in the world with main span of 1088 m. The pile cap is 113.8 m by 48.1 m by 13.3 m under each pylon and the foundation is super-long large-diameter drilled pile groups consisting of 131 piles with the length of 114/117 m and the diameter of 2.8/2.5m. This paper presents the static loading tests on single piles, centrifugal model tests on pile groups, finite element analysis, cap model tests and field monitoring for the super-large scale pile foundation. The results show that: the super-long large-diameter bored pile of Sutong Bridge is floating piles, and it is difficult for the resistance at pile bottom to play. based on the comprehensive consideration of theoretical calculation, centrifugal model tests and finite element analysis, the pile group effect coefficient of the Sutong Yangtze Bridge is 0.82. The pile-head load distribution of pile foundation under main bridge pylon presents a "W" shape, which is larger at both the edges and intermediate connection and smaller at other position of pylon. According to the results of cap model tests, the soften-coordinated spatial truss model was suitable for the stress analysis of cap. The calculated results agree well with the field monitoring results.

1 INTRODUCTION

1.1 Project Outline

Sutong Yangtze River Bridge is located in the southeast of Jiangsu Province, connecting the cities of Nantong and Suzhou. It is a key project to cross the Yangtze River for the national trunk highway from Shenyang (a city in north China) to Haikou (a city in south China) and also an important part of trunk highways in Jiangsu Province. Sutong Bridge has a total length of 32.4 km, the part across Yangtze river is 8146 m, consisting of northern approach bridge (3485 m), main bridge (2088 m), auxiliary bridge (923 m) and southern approach bridge (1650 m). The main bridge is a seven-span continuous steel box girder cable-stayed bridge with the span arrangement of 100m+100m+300m+1088 m+300m+100m+100m=2088m.

Sutong Bridge construction created four world records: the largest foundation, with 113.8 m by 48.1 m pile caps and 114/117 m long piles; the highest pylon - 300.4m; the longest stayed cable 577 m； and the largest main span 1088 m. Sutong Bridge is located at the Nantong section of the downstream part of the Yangtze River，about 108 km away from the Yangtze River estuary in the east. The site is characterized by complicated construction conditions. The bed rock is buried very deep. The thickness of cover layer at bridge site is over 270 m, mainly consisting of clay, silty clay and silty sand etc. Good bearing layer is below -80 m. The riverbed mainly consists of silt and silty sands and is overwhelmingly subject to scour. In order to make foundation safe, reduce cap weight and improve cap bearing, at the same time as much as possible to improve the bearing capacity of pile group, the super-large dumbbell-shaped cap and super-long large-diameter pile group foundation with 131 bored piles were designed after optimization (shown in Fig.1 and Fig.2).

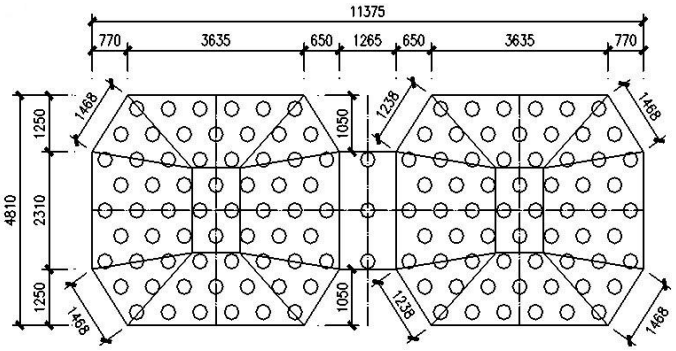

Fig.1. Layout of north pylon foundation for Sutong Bridge

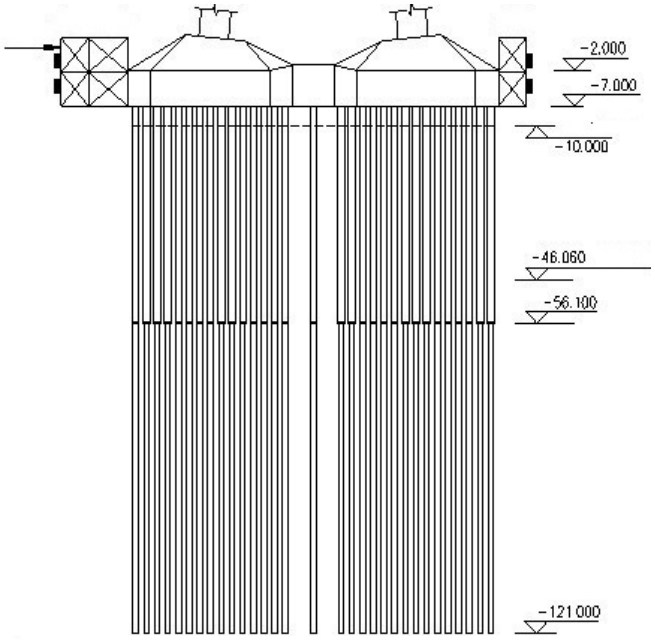

Fig.2. Construction of main bridge the South pylon pile group foundation (units:m)

1.2 Geological Conditions

The main pylon foundation is the super-long large-diameter bored pile group foundation. The upper diameter and lower diameter of pile is 2.8m and 2.5m respectively. The length of bored pile of the North foundation (the 4th main pier) and the South foundation (the 5th main pier) is 117m and 114m respectively.

The geological conditions of Sutong bridge main pier are as follows: distribution of soft soil is very thick, and no rock stratum can be used for bearing stratum in 270m. According to geological age, genetic type, lithology, burial conditions as well as physical and mechanical characteristics of the bridge district, the bridge district can be divided into 22 engineering geological strata, and the main physical and mechanical indexes of 5th pylon foundation stratum was given only as shown in Table 1.

Table 1 Main physical and mechanical indexes of soil of main 5th pylon Foundation

Pleistocene	Stratum No.	Soil name	Natural moisture W (%)	Natural density ρ (g/m^3)	Natural pore ratio e	Liquid limit I_L	Plastic limit I_P	Compressive modulus E_s (MPa)	Unconfined compressive strength q_s (KPa)	Blow count of standard penetration test N
Q4	3-1	Silty clay loam	40.6	1.79	1.122	36.1	20.8	3.52		4.3
	3-3	Clay loam	35.6	1.78	1.09	34.1	20.4	3.28	25.83	11
	4-1	Silty clay loam	40.6	1.74	1.187	33.8	20.6	2.77	8.67	11.8
	4-2	Clay loam	33.1	1.83	0.988	31.9	19.8	3.98	44	17
Q3	5-2	Silty fine sand	25	1.96	0.721			13.35		35.9
	5-	Clay loam	30.7	1.88	0.832	31.4	20.4	8.4		26.1
	6-1	Coarse sand with gravel	13.9	2.12	0.44			23.95		38.4
	6-2	Silty fine sand								59.1
	7-1	Silty fine sand	19.3	2.01	0.593			13.68		54.5
	8-1	Coarse sand with gravel	11.6	2.15	0.383			18.91		73.3
	8-2	Silty fine sand	Sand	17.1	2.04			11.17		58.7
Q2	9	Clay loam and clay	23.5	2.05	0.646	37.5	20.1	9.44	445	60.3
	10	Silty fine sand	19.4	1.99	0.596			10.48		64.5
	11	Clay loam and clay	24.6	2.02	0.687	37	20.5	8.63	432	70.5
	12	Silty fine sand	18.7	2.07	0.532			16.75		
	13	Clay loam and clay	26.3	1.99	0.734	33	17.6		466	
	14	Fine sand	23	1.98	0.675			12.57		

2.STATIC LOADING TESTS OF SINGLE PILE

2.1 Test Method

A total of 17 static loading tests of single pile were carried out by four phase pile tests, one of the piles (N1 pile in the 1st phase) was tested by anchor-pile method, the other 16 piles were tested by O-cell method [1].

The O-cell method was used in static loading tests to determine the larger ultimate bearing capacity of super-long large-diameter pored pile, in which reliable design basis was provided for engineering design and effect of post grouting was tested effectively.

2.2 Test Results

The pile parameters and test results by four phases are listed in table 2, and the curves between load versus displacement at pile top of all test piles are shown in Fig.3.

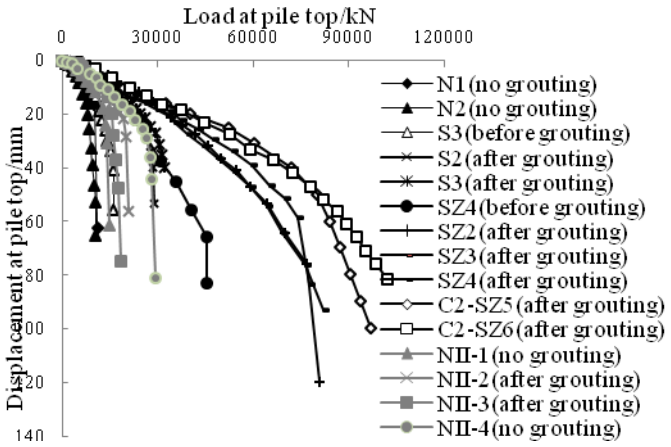

Fig.3. Comparison of curve between load and displacement at pile top of all test piles

Table 2 Bearing Characteristics of All Piles under Ultimate Load in Four Phases

Phase No.	Pile No.	State	Pile diameter (m)	Pile length (m)	Ultimate load P_u (kN)	Displacement (mm)	Ultimate load at pile bottom P_{bu} (kN)	P_{bu}/P_u (%)	Displacement/ Pile diameter (%)
1st	S1	Before grouting	1.50	76	24379	41.52	3242	13.30	2.77
		After grouting			42000	52.95	13424	31.96	3.53
	S2	After grouting	1.50	76	28616	40.36	5421	18.95	2.69
	S3	Before grouting	1.50	76	15970	40.09	1466	9.18	2.67
		After grouting			32109	39.62	8156	25.40	2.64
	N1	No grouting	1.00	84	10000	16.72	0	0	1.67
	N2	No grouting	1.00	69	10501	52.75	555	5.29	5.28
	N3	Before grouting	1.80	69	26007	65.98	4417	16.97	3.67
		After grouting			42020	56.52	11679	27.79	3.14
2nd	SZ2	After grouting	2.8/2.5	125	77051	75.91	14656	19.02	3.04
	SZ3	After grouting	2.8/2.5	106	73991	58.50	30761	41.57	2.34
	SZ4	Before grouting	2.8/2.5	125	44569	64.57	8485	19.04	2.59
		After grouting			82168	92.65	33375	40.62	3.71
3rd	C1-SZ2	After grouting	2.8/2.5	114	103839	65.07	36312	34.97	2.60
	C2-SZ5	After grouting	2.8/2.5	126	96800	100.00	12000	12.40	4.00
	C2-SZ6	After grouting	2.8/2.5	126	101818	82.18	33085	32.49	3.29
	C2-SZ7	After grouting	2.8/2.5	117	107248	74.92	38571	35.96	3.00
4th	NII-1	No grouting	1.2	58.9	14037	29.79	2161	15.39	2.48
	NII-2	After grouting	1.2	58.9	20075	28.18	4583	22.83	2.35
	NII-3	After grouting	1.5	63.6	28349	44.11	7717	27.22	2.94
	NII-4	No grouting	1.5	63.6	17629	48.53	2543	14.42	3.24

According to the tests by four phases, it is concluded that:

1. In the first phase tests, the test results of pile N1 by anchor-pile method are close to that of pile N2 by O-cell method, it is verified that the O-cell method is feasible and reliable.

2. The ultimate load at pile bottom of super-long piles accounts the global ultimate load for 10~20%, and the largest value is 35.96% among the all pile tests. The compression of super-long bored pile should not be overlooked. Under the ultimate load, the compression of piles accounts the displacement at pile top for 15~40% before grouting, and for 30~40% after grouting.

3. Post Grouting at pile bottom will not only improve the base resistance, but also improve the side resistance. Before grouting the side resistance accounts the ultimate load for 85.77~93.04%, while the ratio of side resistance to ultimate

load is 77.86~65.33% after grouting. The improvement of side resistance contributes to the improvement of the total ultimate bearing capacity 56%~88%.

3 CENTRIFUGAL MODEL TESTS

The centrifugal model tests were carried out on 18-pile group, foundation of one-second main bridge (64-pile group) and full bridge pylon under vertical load (131-pile group). The ground maximum scour depth and full grouting at pile bottom were considered, and the tests models are shown in Fig.4 [2].

Fig.4. Centrifugal model test

3.1 Simulation of Soil, Pile and Pile Bottom

The representative soil strata were selected to simulate the Sutong Bridge foundation soil, and the foundation material of model was entirely taken from the field soil. Main properties of model foundation soil are listed in table 3.

Table 3. Main Property of Model Foundation Soil

Pleistocene	Typical elevation	Type of soil	Moisture W%	Density ρ (g/m^3)	Undrained shear strength S_u (kPa)
Q4	Above -51.8m	Clay loam	35	1.81	25
	-95.6m~ -51.8m	Silty fine sand	22	2.00	57
Q3	-95.6m~ -127.9m	Medium sand	13	2.12	90
Q2	Below -127.9m	Clay loam	23	2.05	71

Key issues in simulation of piles are that the deformation properties of pile should be consistent with the prototype, and the friction properties between pile and soil around pile should also be the same as the prototype. Based on centrifugal model similar rates the concrete pile with diameter of 17.5/15.6mm should be used for model piles, but it is difficult to product. Therefore, the aluminum alloy tube was used for model piles, with elastic modulus about 70 GPa.

Post-grouting at pile bottom was used for Sutong bridge main pier pile. However, simulation of post-grouting at pile bottom in centrifugal model test is very difficult. In advance production of soil-cement column was used for the model test to the simulation of post-grouting, the compressive strength of which is 400kPa. For ease of analysis the pile number of pile group of main bridge pylon are shown in Fig.5.

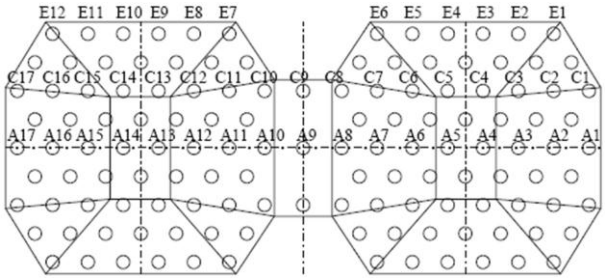

Fig.5. Pile number of pile group of main bridge pylon

3.2 Variation Rules of Load at Pile Top

The load at pile top in pile group increases linearly with the increasing of load on cap, but the increasing degree of load at different pile top is very different. The increasing degree of the load at pile top located at the corner of cap is significantly greater than that of the center pile of cap. With increasing of load on cap, the axial load at pile top in the center of cap both sides increase linearly at the beginning, the curve of axial load at pile top versus load on cap warp up gradually when the load reaches a certain value. After reaching another certain value, the load on cap continue to increases linearly. The side piles and corner piles at both side of dumbbell-shaped cap increase linearly at the beginning with increasing of load on cap, the axial load at pile top versus load on cap curve warp down gradually when the load reaches a certain value. The variation of axial load on center, side and corner piles with load on cap are respectively as shown in Fig.6~8.

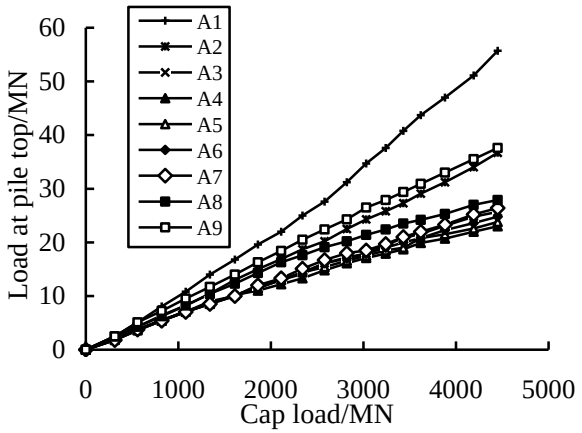

Fig.6. Load variation at pile top of array A in main bridge pylon pile group foundation with load on cap (full grouting and maximum scour depth)

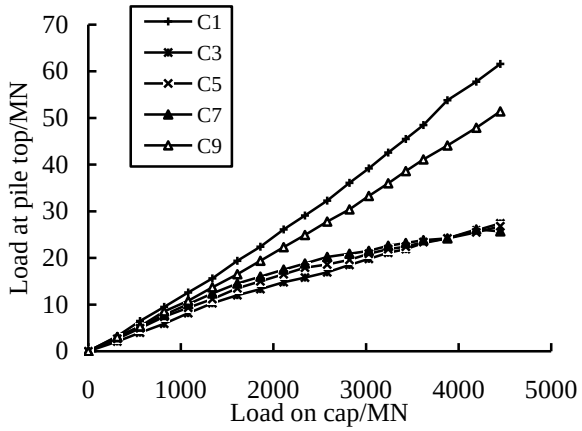

Fig.7. Load variation at pile top of array C in main bridge pylon pile group foundation with load on cap (full grouting and maximum scour depth)

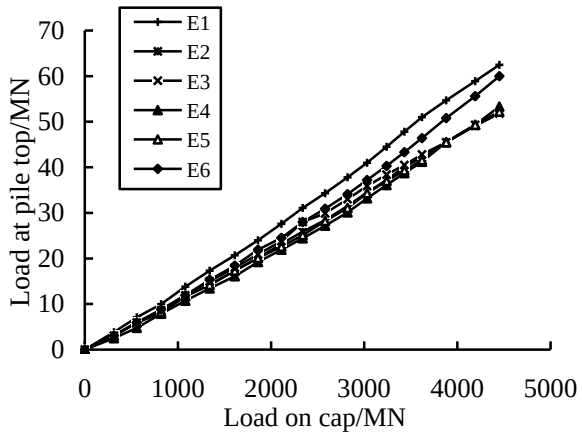

Fig.8. Load variation at pile top of array E in main bridge pylon pile group foundation with load on cap (full grouting and maximum scour depth)

3.3 Load Distribution at Pile Top

The pile-soil interaction degree in different location effected by soil around is different, which makes its deformation characteristics also different. Therefore, the load distribution of main bridge pylon pile group foundation presenting "W" shape is large at both edge and middle connection as well as small in other location under pylon (shown in Fig.8 to Fig.10). With the load increasing at cap, the load at pile top increases, and the ratio of load to the average load at pile top also varies accordingly. Under the same load at cap, axial load at pile top of cap inside is smaller than that of cap edge in the same array piles. The axial load at pile top becomes larger with increase of distance from pile to axis of transverse bridge at the same distance from pile to the axis of longitudinal bridge.

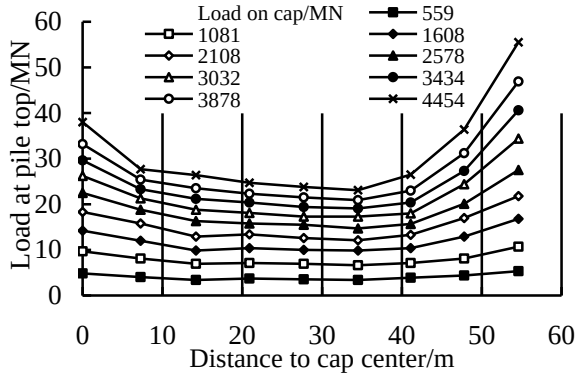

Fig.9. Load distribution at pile top of array A in pile group foundation (full grouting and maximum scour depth)

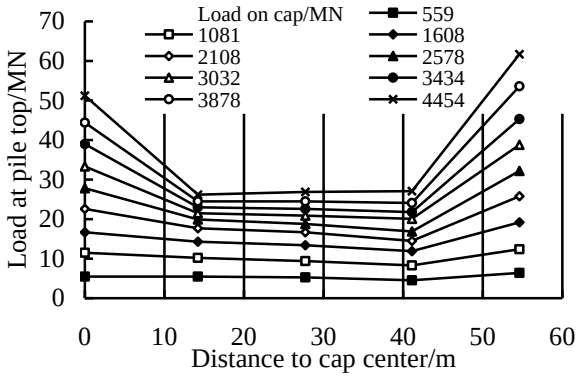

Fig.10. Load distribution at pile top of array C in pile group foundation (full grouting and maximum scour depth)

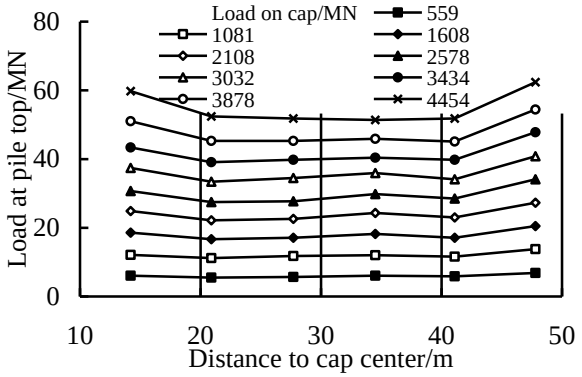

Fig.11. Load distribution at pile top of array E in pile group foundation (full grouting and maximum scour depth)

4 PILE GROUP EFFECT COEFFICIENTS CALCULATION

The overall bearing capacity of pile group is not simply equal

to the superposition of single piles. Such characteristic of pile group different from single pile is defined the pile group effect, and which can be reflected by pile group effect coefficients according to research results of others. In this paper pile group effect coefficients η was defined as follows:

$$\eta = \frac{\text{Ultimate load of pile goup}}{\text{Ultimate load of single pile} \times \text{Number of pile}} \quad (1)$$

4.1 Theoretical Calculation

The failure of pile group foundation of Sutong Bridge belongs to the overall damage [3]. The bearing capacity of such pile group could be calculated by the equivalent pier foundation and reduction calculation method considering pile group effect [4,5].

In this paper the pile group effect coefficients of Sutong Bridge are calculated based on foundation soil stress superposition. The results by this method and centrifugal test are listed in Table 4. The pile group effect coefficients by theoretical calculated results are 7.2 to 12.7% smaller than that by centrifugal tests. Therefore, the two methods are verified by each other.

Table 4. Pile Group Effect Coefficients Comparison with Different Pile Arrangement and Spacing

Pile number	4	9			18	64
Pile Arrangement	rectangle	rectangle			Plum blossom	Plum blossom
Pile Spacing	2.5d	2.5d	4.0 d	6.0d	2.5d	2.5d
Pile group effect coefficients by centrifugal test	0.883	0.853	1.063	1.126	0.870	0.820
Pile group effect coefficients based on Stress superposition	0.819	0.768	0.935	0.983	0.846	0.788

4.2 Finite Element Calculation

The pile group effect coefficients were calculated by the three dimensional finite element procedures TDAD. The three-dimensional mesh was divided in the height direction, at the same time, the distribution of strata was taken into account. The strata scope of finite element calculation is above the elevation of -220m (including the strata above ground maximum scour) and 110m around cap in the lateral direction. According to in-situ tests and numerical simulation, the effects of soil above the maximum scouring line on pile cannot be ignored. Therefore, the parts of soil above the scour line was also calculated together with taking the effect of the riverbed filled protective layer (15m). The three-dimensional finite element meshes of South pylon pile foundation are shown in Fig.12.

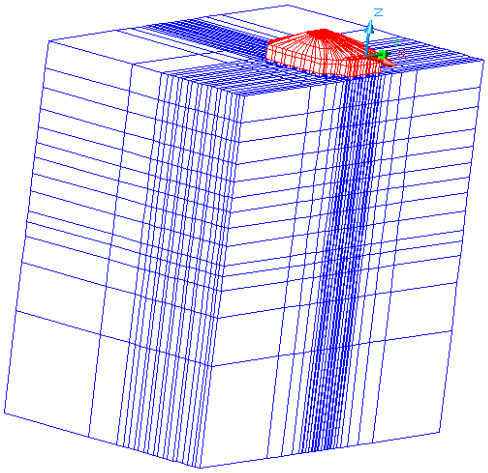

Fig.12. Three-dimensional mesh of South pylon foundation

Concrete was taken into consideration as a linear elastic material in calculation. The elastic modulus of concrete in cap and piles is 31.5GPa and 33GPa. Both the Poisson's ratio of concrete is 0.167, and unit weight is 24kN/m^3. As part of cap immersed in water, therefore, the concrete in cap and piles below the water level -2.0m were calculated by float density. The Duncan-Chang model was used for simulation of soil. Based on the triaxial consolidation drainage, direct shear and compression test of soil and so on, the model parameters were determined comprehensively after similar stratum merged, and the parameters of the Duncan-Chang model of pile group foundation are listed in Table 5.

Table 5. The parameters of the Duncan-Chang model of pile group foundation

Stratum No.	Soil type	Elevation of stratum top and bottom (m)	R_f	K	n	G	F	D	φ (^{0})	C t/m^2	ρ t/m^3
1	Clay loam	-27.0～-12.0	0.74	321.2	0.61	0.38	0	0	31.3	2.4	0.98
2	Clay loam	-38.0～-27.0	0.74	321.2	0.61	0.38	0	0	31.3	2.4	0.98
3	Clay loam	-50.0～-38.0	0.74	321.2	0.61	0.38	0	0	31.3	2.4	0.98
4	Silty fine sand	-60.0～-50.0	0.7	477	0.55	0.4	0	0	29.9	2	1.04

5	Silty fine sand	-69.0～-60.0	0.7	477	0.55	0.4	0	0	29.9	2	1.04
6	Coarse sand with gravel	-77.0～-69.0	0.81	522	0.63	0.4	0	0	33.2	1.9	1.1
7	Silty fine sand	-86.0～-77.0	0.7	477	0.55	0.4	0	0	29.9	2	1.04
8	Silty fine sand	-96.0～-86.0	0.7	477	0.55	0.4	0	0	29.9	2	1.04
9	Coarse sand with gravel	-107.0～96.0	0.75	668.1	0.55	0.4	0	0	34.1	1	1.19
10	Silty fine sand	-113.0～-107.0	0.8	516.3	0.58	0.4	0	0	31.2	1.9	1.18
11	Silty fine sand	-121.0～-113.0	0.8	516.3	0.58	0.4	0	0	31.2	1.9	1.18
12	Clay loam and clay	-136.0～-121.0	0.8	376	0.59	0.38	0	0	33.7	2.95	1.08
13	Silty fine sand	-163.0～-136.0	0.7	477	0.55	0.4	0	0	29.9	2	1.04
14	Clay loam	-220.0～-163.0	0.69	368.1	0.53	0.38	0	0	28.2	5	1.04
15	Pile-soil interface		0.7	300	0.62	0.35	0	0	22.5	1	1.1
16	Grouting material at pile bottom		0.78	497	0.5	0.3	0	0	33.9	1	1.1
17	Grouting material interface		0.78	497	0.5	0.3	0	0	24.0	10	1.1
18	Protective layer		0.74	1800.0	0.4	0.38	0	0	40.0	2	1.1

The pile group effect coefficients of number of 1, 2, 3, 4 and 7 pile were analyzed by Finite Element method. According to pile spacing and arrangement, a total of 11 cases were analyzed, and pile group number, number of pile and pile spacing were listed in Table 6.

Table 6. Ultimate Load and Pile Group Effect Coefficients

Ultimate displacement (mm)	Pile group number	1-1	2-1	2-2	3-1	3-2	4-1	4-2	4-3	7-1	7-2	7-3
	Number of pile	1	2	2	3	3	4	4	4	7	7	7
	Pile spacing (×d)	2.41	2.41	4.82	2.41	4.82	2.41	4.18	4.82	2.41	4.82	7.23
75	P_u (MN)	103.3	97.3	100.9	81.1	93.3	76.8	90.2	93.2	52.5	72.1	87.4
	η	1.000	0.942	0.977	0.785	0.903	0.743	0.873	0.902	0.508	0.698	0.846
60	P_u (MN)	94.3	85.0	90.72	68.56	80.27	63.8	75.9	78.9	43.4	59.0	72.4
	η	1.000	0.901	0.962	0.727	0.851	0.677	0.805	0.837	0.460	0.626	0.768
80	P_u (MN)	106.3	100.3	103.9	85.0	97.1	80.9	94.4	97.0	55.5	76.1	91.8
	η	1.000	0.944	0.977	0.800	0.913	0.761	0.888	0.913	0.522	0.716	0.864
40	P_u (MN)	79.3	62.0	68.0	48.8	57.8	44.5	52.8	54.8	30.0	40.4	49.7
	η	1.000	0.782	0.858	0.615	0.729	0.561	0.666	0.691	0.378	0.509	0.627

Based on the comprehensive consideration of theoretical calculation, centrifugal model tests and finite element analysis, the pile group effect coefficient of the Sutong Yangtze Bridge is 0.82.

5 CAP TESTS

5.1 Model Tests

In order to research the failure modes of large cap with pile group foundation and verify the reliability of spatial truss model, a total of 12 models were designed by scale ratio of 1:10, including 10 nine-pile and 2 sixteen-pile cap (CT1-CT12). Nine-piles cap specimen CT1, CT2, CT3, CT4 and 16-pile cap specimen CT11, CT12 were analyzed only in this paper. The main parameters of test models are cap height (aspect ratio), loading types, rates of reinforcement and reinforced pattern. Geometry and reinforcement of specimens are listed in Table 7. The test setups are shown in Fig.13.

Table 7. Geometry and reinforcement of specimens

Specimen number	Cap geometry			P	Note
	D/h_0 (mm)	S (mm)	H/h_0 (mm)		
CT1	1.76	450	360/307	0.54	Uniform reinforcement
CT2	2.21	450	300/245	0.61	Centralized reinforcement and L4 reinforcement mat at cap bottom
CT3	1.77	450	360/306	0.55	
CT4	1.44	450	420/375	0.52	
CT11	1.82	300	360/315	0.54	
CT12	1.55	300	400/350	0.53	

Note: D is the closest distance of pile side to the longest pile

center, h_0 is effective height of cap specimen, S is the distance of pile center to adjacent pile center, H is cap height, and unidirectional longitudinal tensile main reinforcement ratio $P=100A_s/(bh_0)$

Fig.13. Testing setup (9-pile and 16-pile)

The crack development of nine-pile and 16-pile cap specimens are shown in Fig.14. All cap specimens were with centralized reinforcement except specimen CT1. From the test the thickness of cap specimen CT4 is 120mm and 60mm thicker respectively than that of cap specimen CT2 and CT3. Under the almost reinforcement ratio, the cracking load of cap specimen CT4 increased 200% and 186%, and the ultimate load of which increased 183% and 157%. It is indicated that the effects of thickness increasing of cap specimen are obvious.

Under the same condition the ultimate load of CT3 is 1.1 times larger than CT1, it is explained that centralized reinforcement is more in accordance with force transferring mode of spatial truss. Centralized reinforcement at cap top could undertake effectively the tensile load at cap bottom. Therefore, the bearing capacity of cap were improved.

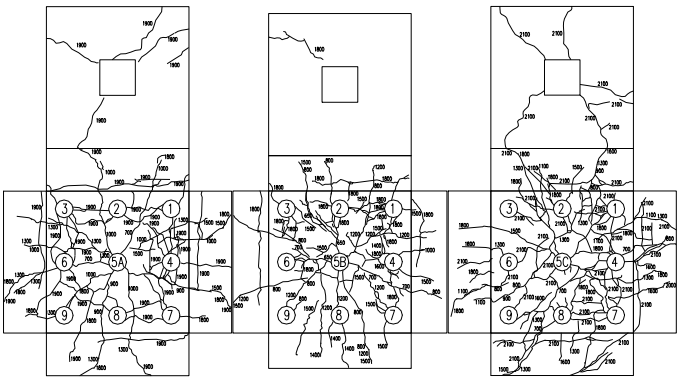

(a) CT1 *(b) CT2* *(c) CT3*

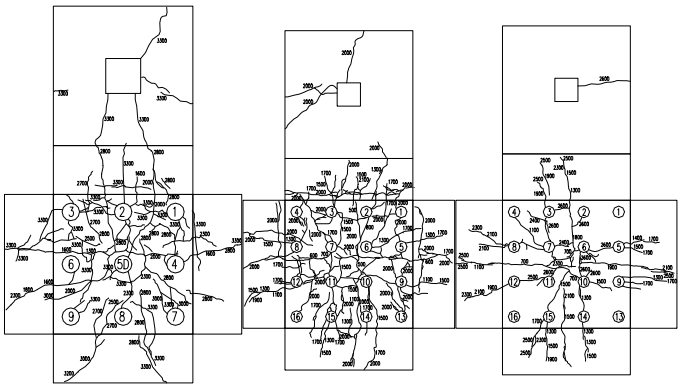

(d) CT4 *(e) CT11* *(f) CT12*

Fig.14. Crack development of all nine-pile and 16-pile cap specimens

The thickness of specimen CT11 and CT12 with centralized reinforcement is 360mm and 400mm respectively (the aspect ratio is 1.55 and 1.82). The ultimate load of specimen CT12 is 1.3 times larger than that of specimen CT11, It is also verified that the thickness increasing of cap is in favor of bearing capacity of cap.

The thick caps were analyzed by the softened truss model and reinforced concrete shear cell theory [6]. After the compression yield criterion of the model modified due to the tensile contribution of concrete, the softening coordination spatial truss model used to calculate pile foundation cap bearing capacity was established. The test and calculated results of cracking and failure load were listed in Table 8. The calculated results agree well with the experimental results.

Table 8. Cracking, failure and predicted load of cap specimen

Specimen		CT1	CT2	CT3	CT4	CT11	CT12
Cracking load	Test results	700	650	700	1300	500	700
	Calculated results	797	483	765	1157	734	806
Failure load	Test results	1900	1800	2100	3300	2000	2600
	Calculated results	2016	1687	2368	3310	2278	2872
	The average and variance of ratio of predicted results to test results is 1.062 and 0.079 except cap with concrete only and less-reinforced.						
Predicted load		1389	1062	1523	2169	1479	1616

5.2 Field Space Truss Tests

The monitoring equipment was set in the downstream cap of 4# pier of Sutong Bridge. Due to the plane dimensions and the distribution of vertical load symmetrical roughly, the one-fourth size of downstream cap was studied only. A total of 25 steel stress sensor was set up to test the tension stress of oblique compression bars and cap bottom. Steel stress sensors

is vibrating wire steel stress sensor, and the test data collection of cap was carried out by 4 phases. The 1st phase is when cap concrete casting was completed (May 10, 2005). The 2nd phase is when lower beam concrete casting is completed (November 29, 2005). The 3rd phase is when cable pylon concrete casting is completed (October 31, 2006). The 4th phase is when 7# steel box girder lifting is completed (December 22, 2006). Measurement points Layout of reinforcement mesh at cap bottom are shown in Fig.15, and layout of field steel bar sensor on downstream cap of 4# pier are shown Fig.16.

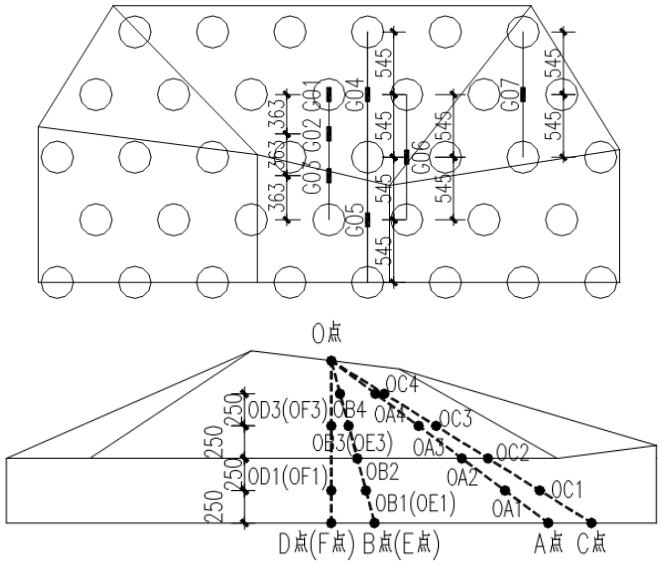

Fig.15 Measurement points layout of reinforcement mesh

Fig.13. Layout of field steel bar sensor on downstream cap of 4# pier

The strain variation at cap bottom was shown in Fig.14. Due to the field test load much smaller than ultimate bearing capacity of cap, the effects of spatial trusses is not obvious. Due to effects of hydration heat or tidal, the strain increase first, and then reduce. From the whole trend the cap bottom is in the tensile state.

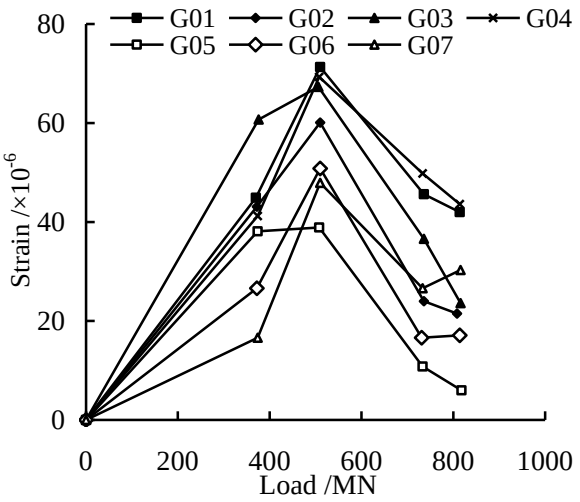

Fig.14. The strain curves of steel at cap bottom

6 CONCLUSIONS

According to the results of single pile tests, centrifugal model tests of pile group, numerical simulation, field detecting and laboratory experiments of cap spatial truss model, it is concluded that:

1. The test of bearing capacity of super-long large-diameter bored pile was determined by combination of O-cell test method and anchor piles, which provides a reliable basis for the project design and a valuable analysis data for scientific research.

2. According to the test results, the super-long large-diameter bored pile of Sutong Bridge is floating piles, and it is difficult for the resistance at pile bottom to play. The compression of super-long bored pile should not be overlooked. The compression of pile after grouting account total displacement at pile top for 30~40%.

3. The pile-cap-soil interaction was analyzed by centrifugal model test and numerical simulation, load distribution of pile top was obtained, both of which have guiding significance for design in future.

4. The pile group effect coefficients with different pile spacing and arrangement were studied by centrifugal tests, theoretical method and finite element analysis, the pile group effect coefficient of the Sutong Yangtze Bridge is about 0.82.

5. The cap with pile group were studied by model and field spatial truss tests, and the cracking, ultimate load of cap specimens were calculated by softening coordination spatial truss model. The calculated results are consistent with test results.

According to theoretical analysis, numerical simulation, field tests as well as centrifugal model tests and so on, it is concluded that cap with pile group foundation of Sutong bridge are safe and reliable.

ACKNOWLEDGEMENTS

The research was supported by the National Natural Science Foundation of China (Grant No.50908048) and a project funded by the Priority Academic Program Development of Jiangsu Higher Education Institutions (PAPD).

REFERENCES

[1] Southeast University [2004], "*General report of pile tests of Sutong Bridge* "

[2] Weiming Zhang, Lianxiang Wang [2004], " *Centrifuge model study of foundation-soil interaction of Sutong Yangtze River highway Bridge* "

[3] Daohua Hu and Anfu Deng [1997]. " *Study of bored pile group bearing characteristic* ". Natural gas and oil, Vol., I, No. 15, pp. 46-50

[4] Tao Xie, Wenzhong Yuan and Yong Yao [2003]. " *Model test study on effect of vertical bearing capacity for large scale pile group* ". Journal of highway and transportation research and development, vol., V, No. 20, pp. 61-64 (In chinese)

[5] Xiangyu Wang, Chenghua Wang and Shaofei Li [2003]. " *Discussion with regard to the equivalent deep foundation method in calculating bearing capacity of grouped piles* ". Port engineering technology, No.4, pp. 42

[6] Suzuki K., Otsuki K. and Tsubata T [1998]. " *Influence of bar arrangement on ultimate strength of four-pile caps* ". Transactions of the Japan Concrete Insititute, No. 20, pp. 195-202